

IN VITRO EVALUATION OF HEPATIC AND EXTRA-HEPATIC METABOLISM OF COUMARINS USING RAT SUBCELLULAR FRACTIONS: CORRELATION OF *IN VITRO* CLEARANCE WITH *IN VIVO* DATA

Dayanidhi Behera¹, Anagha Damre^{2*}, Alice Varghese²
and Veeranjanyulu Addepalli¹

¹*School of Pharmacy and Technology Management, NMIMS
University and* ²*Drug Metabolism and Pharmacokinetics, Piramal
Life Sciences Limited, Goregaon (E), Mumbai, India*

SUMMARY

7-Ethoxycoumarin (7-EC) and 7-hydroxycoumarin (7-HC) were chosen as model compounds to study hepatic and extra-hepatic metabolism in rat tissue subcellular (microsomal and S9) fractions and to scale the observed *in vitro* clearance to *in vivo* plasma clearance. 7-EC and 7-HC showed significant metabolic degradation in liver subcellular fractions as compared to subcellular fractions obtained from intestine, kidney, lung and brain. The total *in vitro* metabolic clearance for 7-EC and 7-HC was determined by adding the individual *in vitro* organ clearance values obtained in hepatic and extra-hepatic microsomes or S9 fractions. The predicted *in vivo* clearance for 7-HC was 63.6 and 81.6 ml/min/kg by *in vitro* scaling from microsomes and S9 fractions, respectively. For 7-EC, the values were 78.5 and 76.8 ml/min/kg, respectively. The predicted clearance was found to be reasonably accurate with slight over- and underprediction. Interestingly, the relative contribution of hepatic and extra-hepatic metabo-

* Author for correspondence:

Dr. Anagha Damre

Drug Metabolism and Pharmacokinetics

Piramal Life Sciences Limited

Goregaon (E)

Mumbai-400 063, India

e-mail: anagha.damre@piramal.com

lism to the total clearance of 7-EC and 7-HC was remarkably high, ranging from 62-77% and 22-38%, respectively, of the total metabolic clearance. It is concluded that the model of multi-organ subcellular fractions is a useful *in vitro* tool for the prediction of *in vivo* metabolic clearance, as it can provide information about the relative contribution of extra-hepatic and hepatic metabolism to total metabolic clearance.

KEY WORDS

intrinsic clearance, organ clearance, cytochrome P450, scaling, 7-ethoxycoumarin, 7-hydroxycoumarin

INTRODUCTION

Although the liver plays a major role in xenobiotic metabolism, drug-metabolizing enzymes are also present in other organs. Thus, other organs, such as lungs, kidneys, intestine and brain, can contribute significantly to biotransformation of compounds in the body and can play a role in total metabolic body clearance, and should be considered in any discussion of drug disposition.

Biotransformation of compounds can be broadly divided into Phase I reactions (oxidation, reduction and hydrolysis) and Phase II reactions (conjugation with glucuronic acid, sulfate, acetate and amino acids) that metabolize compounds into more polar and readily excretable metabolites /1/. In general, these xenobiotic metabolic reactions are regarded as detoxification mechanisms. However, depending on the properties of the compound, bioactivation is also possible, resulting in toxic products. Organ toxicity can, among other factors, be caused by organ-specific metabolism. Cytochrome P450 (CYP) enzymes in extra-hepatic tissues often play a dominant role in target tissue metabolic activation of xenobiotics.

In recent years, several *in vitro* systems have been proposed to predict *in vivo* clearance of drugs. Among the most popular and widely used systems are subcellular fractions, especially microsomes, as they retain the activity of key enzymes involved in drug metabolism that reside in the smooth endoplasmic reticulum, such as CYP, flavin monooxygenases and glucuronosyl transferases /2/, and also because of their predictive utility and ease-of-use. S9 fractions contain both

Phase I and II drug metabolizing enzymes and, therefore, give complete metabolic information of a compound. Tissue slices have the advantage of maintaining a natural interplay between co-factors, transporters and metabolizing enzymes, along with cell-to-cell contacts and intact microarchitecture. However, potential drawbacks also exist, including poor penetration of high turnover drugs into the inner cell layers of slices /3/. Similarly, hepatocytes are widely used in *in vitro* turnover or intrinsic clearance assays; they contain enzymes and co-factors in normal physiological concentrations with the maintenance of cellular integrity /4/. However, they suffer the major drawback of rapid loss of enzyme activity and their cryopreservation process is a challenge /2/.

In the present study, the drug depletion approach was used to determine metabolic clearance of two commonly used model compounds, 7-ethoxycoumarin (7-EC) and 7-hydroxycoumarin (7-HC). 7-EC is a commonly used probe substrate for CYP1A1, CYP1A2, CYP2E1, CYP2A6 and CYP2B6 activity *in vitro* /5/, and it has been recommended as a marker of metabolic competence for a number of *in vitro* systems, including microsomes /6/, isolated hepatocytes /7/, precision-cut liver slices /8/, and various heterologous expression systems /9/. Its initial popularity was based on the fluorescent properties of its metabolite 7-hydroxycoumarin (7-HC), formed by an *O*-deethylation reaction, which allowed the development of a simple, sensitive, and accurate assay procedure /10/. This reaction is catalyzed by a variety of members of the CYP superfamily of enzymes present in both human /9/ and rat /11/ liver. 7-HC formed from 7-EC undergoes Phase II metabolism to predominantly glucuronide and sulfate metabolites (Fig. 1), as well as other reported metabolites, such as 6,7-dihydroxycoumarin /12/. Subcellular fractions supplemented with co-factors can form all these metabolites and therefore can be used to study drug metabolism and intrinsic clearance of 7-EC and 7-HC.

Although the clearance of 7-EC has been well characterized in several *in vitro* systems /13-17/, no investigations have been undertaken to study its clearance in extra-hepatic subcellular fractions. Moreover, it is unclear how important the *O*-deethylation pathway is in the overall metabolic fate of this substrate. Recent studies with rat liver slices indicated that there are a number of other primary

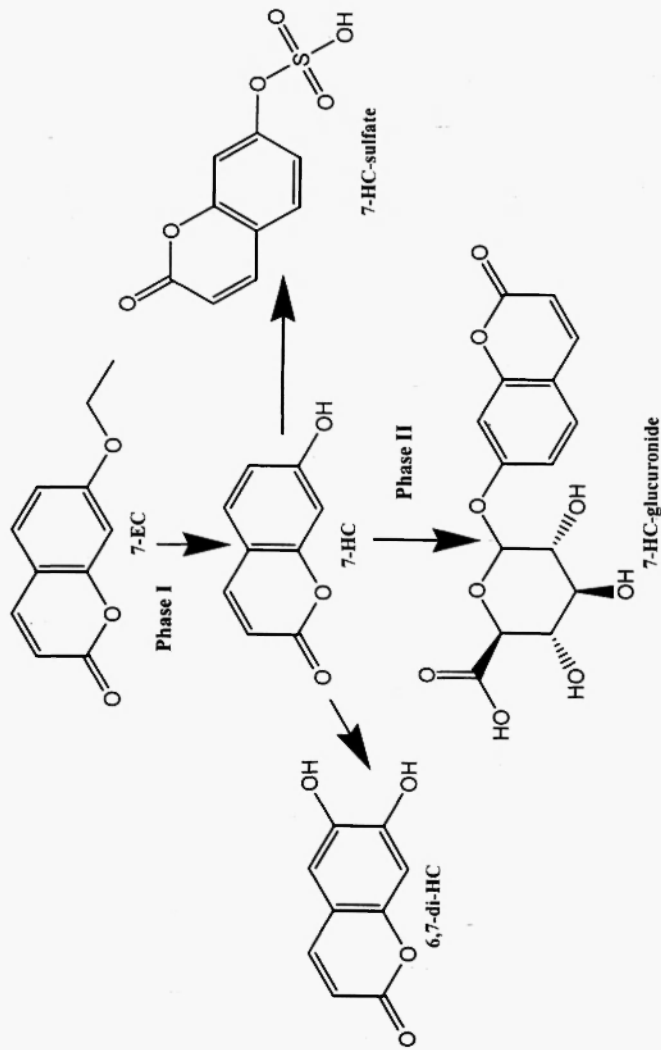


Fig. 1: Pathway of metabolism of 7-ethoxycoumarin (7-EC) and 7-hydroxycoumarin (7-HC). 7-EC undergoes Phase I metabolism to form 7-HC, which further undergoes Phase II metabolism to form 7-HC-sulfate and 7-HC-glucuronide as predominant metabolites, along with 6,7-di-HC.

metabolites of 7-EC /18/. Similarly, the kinetics of 7-HC has not been studied in extra-hepatic subcellular fractions.

Thus, the objectives of the present study were twofold. The first aim was to assess the metabolic stability of 7-EC and 7-HC in hepatic and extra-hepatic subcellular fractions obtained from rats. The second aim was to determine the *in vitro* hepatic and extra-hepatic clearance of 7-EC and 7-HC in subcellular fractions and assess the utility of these *in vitro* systems for prediction of their *in vivo* clearance in rats.

MATERIALS AND METHODS

Materials

Urethane, 7-ethoxycoumarin (7-EC) and 7-hydroxycoumarin (7-HC), β -NADPH (nicotinamide adenine dinucleotide phosphate, reduced tetrasodium salt), UDPGA (uridine 5'-diphosphoglucuronic acid, triammonium salt), PAPS (adenosine 3'-phosphate 5'-phosphosulfate, tetralithium salt tetrahydrate), Trizma base, EDTA (ethylene diamine tetraacetic acid), glycerol, sodium dithionite, Triton X-100, bovine serum albumin and Bradford reagent were obtained from Sigma-Aldrich (Missouri, USA). All other chemicals were of analytical grade and purchased from commercial suppliers.

Animals

Male Wistar rats (250-300 g) bred in-house at Piramal Life Sciences Limited (PLSL), Goregaon, Mumbai, India, were maintained in a temperature- and humidity-controlled room with a 12-h light/dark cycle with free access to standard diet and water. All animals used in this study were mature and healthy and were not subjected to any form of treatment/medication. Guidelines of the Committee for the Purpose of Control and Supervision of Experiments on Animals (CPCSEA), Government of India, were followed and the in-house animal ethics committee approved all experimental procedures.

Preparation of microsomal and S9 fractions

Rats were anaesthetized with intra-peritoneal injection of urethane (1.5 g/kg) and then killed by cervical dislocation. Liver, kidney, intestine, lung and brain tissues were isolated immediately and washed

in chilled isotonic saline to remove excess blood. The adherent connective tissue and fat were removed. Additionally, the intestinal lumen was flushed with isotonic saline to remove partially digested food residues. The tissues were chopped into small pieces and were homogenized with four times their weight in 1.15% potassium chloride with 0.05 M potassium phosphate buffer, pH 7.4, in a tissue homogenizer equipped with a pre-chilled Teflon pestle. The homogenates were centrifuged at 10,000 g for 20 min at 4°C in a refrigerated centrifuge (Sigma 3K30, USA) and the resultant supernatants were separated as S9 fractions. The S9 fractions obtained from each tissue were further subjected to ultracentrifugation (Beckman Coulter, Optima L90K, Class S, UK) at 100,000 g for 1 hour at 4°C and the microsomal pellets and cytosolic fractions were separated. Microsomal pellets obtained from each tissue were resuspended by homogenization in 100 mM Tris-hydrogen chloride containing 20% glycerol and 10 mM EDTA buffer, pH 7.4 (volume [ml] as weight [g] of each organ). The homogenates, isolated S9 fractions and microsomes from each tissue were aliquoted in microcentrifuge tubes and stored at -70°C till further use.

The prepared homogenates, microsomes and S9 fractions were characterized by determining the CYP content using differential spectrophotometric assay as described by Omura and Sato with some modification /19/ and protein content according to Bradford /20/ using a protein assay kit (Bio-Rad Laboratories, Richmond, CA, USA) with bovine serum albumin as the standard.

Microsomal and S9 fraction incubations

The microsomal and S9 incubations for 7-EC and 7-HC were adapted from reported procedures /21,22/. Briefly, reactions were carried out in a final incubation volume of 1,500 µl. Required quantities of liver microsomes and liver S9 fractions were added to sodium phosphate buffer, pH 7.4, on ice, to obtain a final CYP content of 0.5 nmol/ml and a protein concentration of 2 mg/ml. For all other tissues, volumes equivalent to subcellular fractions of liver were used for the incubations. 7-EC or 7-HC was added to obtain a final concentration of 50 µM. For S9 fractions, UDPGA (final concentration, 1.9 mg/ml) and PAPS (final concentration, 1 mg/ml) were added to the reaction mixture. Reactions were initiated by the addition of β-NADPH (final concentration, 10 mM). Immediately after addition of

NADPH, aliquots (100 μ l) were withdrawn for 0 min time. The tubes were then transferred to an incubator shaker adjusted at 37°C and 100 rpm (Max^QMini, Fischer Scientific) for 4 h. Aliquots (100 μ l) were withdrawn at 10, 20, 30, 40, 60, 120, 140, 160, 180, and 240 min from each incubation vial. The aliquots were immediately precipitated with 100 μ l of acetonitrile:methanol (1:1 v/v) solution, vortexed for 2 min and centrifuged at 10,000 rpm (Biofuge, Heraeus) at 4°C for 5 min. The supernatants thus obtained were subjected to HPLC analysis.

HPLC analysis

HPLC analysis was carried out with minor modifications of the method reported previously [23]. Analysis of 7-EC was performed with Thermo Finnigan Surveyor HPLC equipped with a photodiode array (PDA) detector and ChromQuest 4.1 Software. 7-HC was analyzed using Waters Alliance Separation Module 2695 equipped with a PDA detector and Empower Professional software. Analysis was done on a Thermo Hypersil BDS C₁₈ column (250 x 4.6 mm, 5 μ) maintained at 25°C. The mobile phase composition was acetonitrile (A) and 0.01 M ammonium acetate containing 0.5% triethylamine, pH adjusted to 2.5 with orthophosphoric acid (B), with a gradient flow program (time/%A/%B) of 0/0/100, 10/60/40, 18/60/40, 18.01/0/100 and 20/0/100 at a flow rate of 1 ml/min. 7-EC and 7-HC were detected at a wavelength of 320 nm.

Calculation of clearance

The percentage of parent compound remaining at each time point was calculated using Eq. 1:

$$\begin{aligned} &\% \text{ Parent compound remaining} \\ &= (\text{Peak area at } t \text{ min} / \text{Peak area at 0 min}) \times 100 \end{aligned} \quad (1)$$

where peak area at 0 min = concentration of analyte in incubation mixture at 0 minute; peak area at t min = concentration of analyte in incubation mixture at time t minutes.

The slope (k) was calculated from the equation of the graph, $y = kx + c$, obtained by plotting the natural logarithm of the percentage of parent compound remaining against time (min) curve.

Intrinsic clearance (CL_{int}), which is defined as clearance without physiological limitation by blood flow or plasma protein binding, was

determined according to the substrate depletion method with modifications as previously described /24,25/, using Eq. 2:

$$CL_{int} (\mu\text{l}/\text{min}/\text{mg}) = \frac{k \times \text{incubation volume } (\mu\text{l})}{\text{Amount of microsomal protein (mg)}} \quad (2)$$

The CL_{int} obtained was further scaled up to obtain the whole organ intrinsic clearance ($CL_{int,org}$) by multiplying with a scaling factor as described by Trudea-Lame *et al.* with some modification /26/ as shown in Eq. 3. The scaling factor was calculated by determining the protein content of hepatic and extra-hepatic tissue homogenates as mg/g of organ weight.

$$\begin{aligned} CL_{int,org} (\mu\text{l}/\text{min}/\text{kg}) \\ = CL_{int} \times (\text{g liver wt per kg body wt}) \times \text{scaling factor} \end{aligned} \quad (3)$$

To calculate the metabolic organ clearance (CL_{org}) from $CL_{int,org}$, the organ blood flow and the unbound fraction of the compound in plasma *in vivo* (f_u) were considered according to Eq. 4, which is based on the venous equilibration model /3/. The blood flow rates (Q) were obtained from data in the literature /27,28/ as shown in Table 1, and the f_u values for 7-EC and 7-HC used were 0.22 and 0.10, obtained from the literature /29,30/.

$$CL_{org} (\text{ml}/\text{min}/\text{kg}) = \frac{Q \times f_u \times CL_{int,org}}{Q + (f_u \times CL_{int,org})} \quad (4)$$

In addition, the total CL_{org} was calculated by adding the individual organ clearances obtained from respective incubations, as shown in Eq. 5:

$$\begin{aligned} \text{Total } CL_{org} (\text{ml}/\text{min}/\text{kg}) \\ = CL_{liver} + CL_{intestine} + CL_{kidneys} + CL_{lungs} + CL_{brain} \end{aligned} \quad (5)$$

RESULTS

Incubation of 7-EC and 7-HC in rat microsomes and S9 fractions resulted in their significant degradation with time, as shown in Figures 2 and 3. The degradation of both compounds was more pronounced in liver subcellular fractions than extra-hepatic subcellular fractions, illustrating that the liver is the major organ for their metabolism. In

TABLE 1
Scaling factors determined and organ blood flow rates

| Species | Organ | Blood flow* (ml/min/kg body wt) | Organ weight (g/kg body wt) [#] | Organ protein content ^a (mg/g of organ weight) [#] |
|---------|-----------|------------------------------------|---|---|
| Rat | Liver | 55.2 | 47 | 97.9 |
| | Intestine | 30 | 6.3 | 37.1 |
| | Kidneys | 37 | 7.5 | 112.8 |
| | Brain | 5.2 | 5 | 94.3 |
| | Lungs | 1.1 | 4.8 | 75.8 |

[#] Data are presented as mean values (n = 4 for each organ).
* Blood flow data were obtained from the literature [25,27].
The scaling factor ^a was calculated by measuring the protein content of an organ sample with a known wet weight.

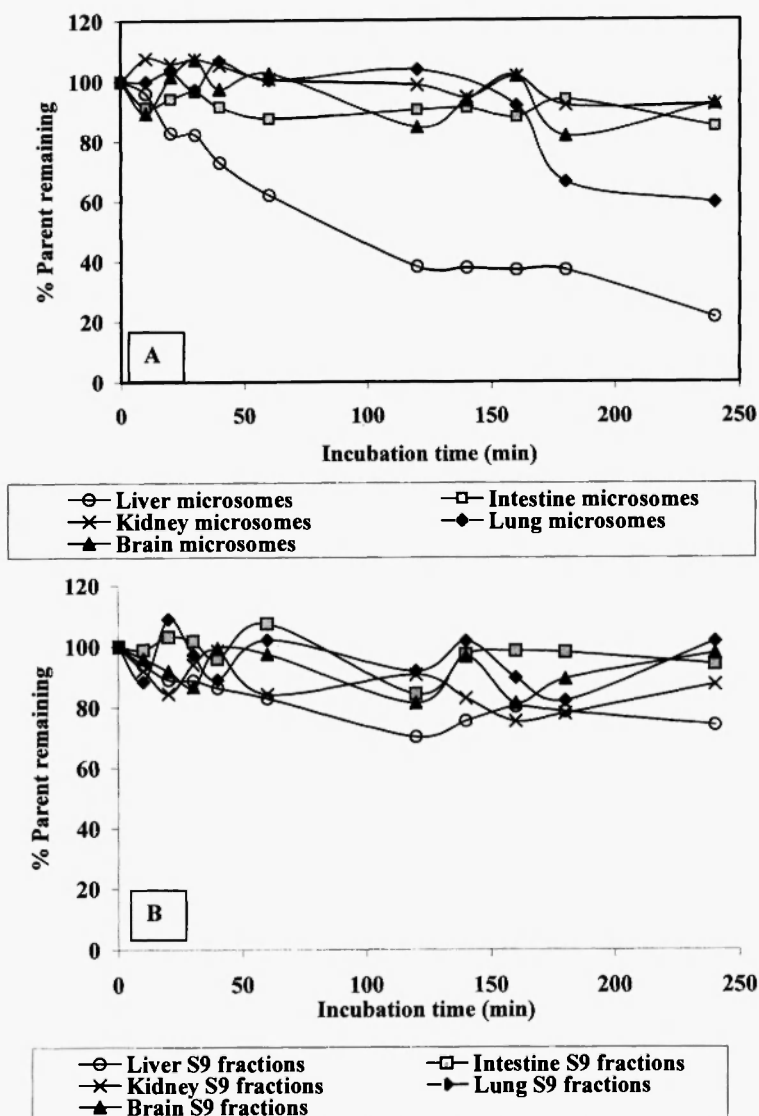


Fig. 2: Metabolic stability of 7-ethoxycoumarin (7-EC) in rat hepatic and extra-hepatic microsomes (A) and S9 fractions (B). 7-EC at a concentration of 50 μ M was incubated in duplicate with rat hepatic and extra-hepatic (intestine, kidneys, lungs and brain) tissue microsomes and S9 fractions for 4 h, which resulted in significant degradation of substrate with time. Samples were aliquoted at 0, 10, 20, 30, 40, 60, 120, 140, 160, 180 and 240 min and analyzed by HPLC to calculate the percentage of 7-EC remaining at each time point with respect to 0 min.

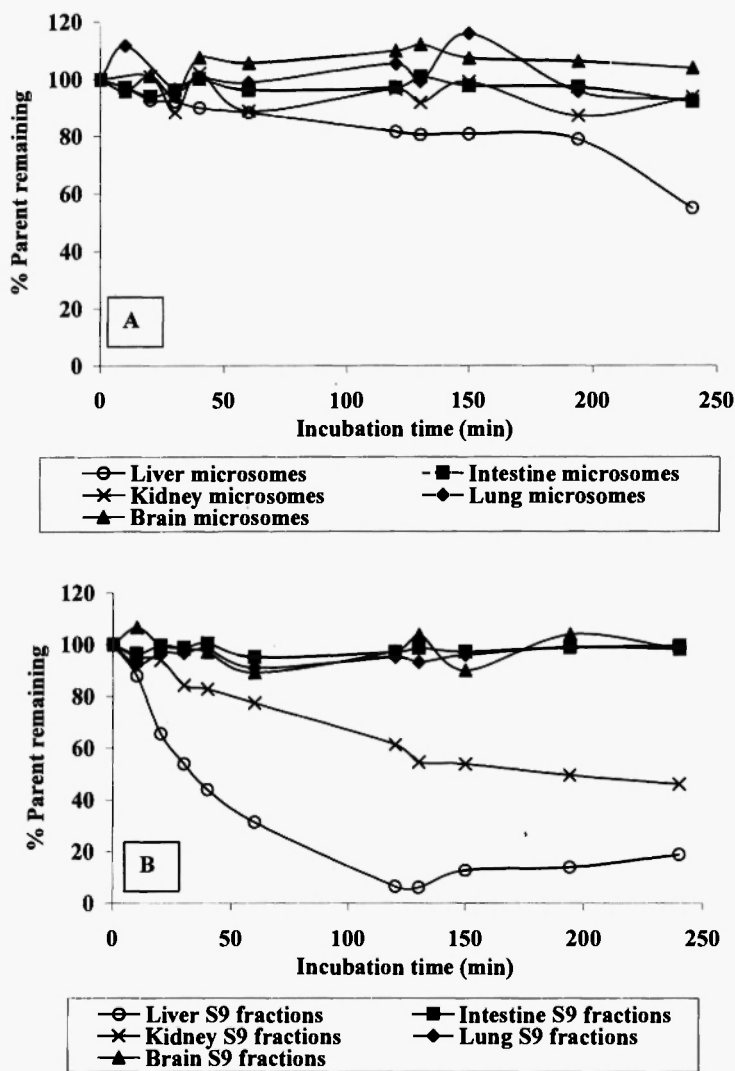


Fig. 3: Metabolic stability of 7-hydroxycoumarin (7-HC) in rat hepatic and extra-hepatic microsomes (A) and S9 fractions (B). 7-HC at a concentration of 50 μ M was incubated in duplicate with rat hepatic and extra-hepatic (intestine, kidneys, lungs and brain) tissue microsomes and S9 fractions for 4 h, which resulted in significant degradation of substrate with time. Samples were aliquoted at 0, 10, 20, 30, 40, 60, 120, 140, 160, 180 and 240 min and analyzed by HPLC to calculate the percentage of 7-HC remaining at each time point with respect to 0 min.

addition, analysis of the metabolites formed revealed a greater number of metabolites in liver subcellular fractions compared to extra-hepatic subcellular fractions, which correlates with degradation studies. Review of the HPLC chromatograms revealed that 7-EC was metabolized into two polar metabolites, M1 (retention time [RT] 10.32 min) and M2 (RT 9.47 min) in rat liver microsomes (Fig. 4). Similarly, in the rat liver S9 fraction, 7-EC was metabolized into three polar metabolites, M1 (RT 11.24 min), M2 (RT 10.20 min) and M3 (RT 8.97 min). The metabolite formed in all incubation mixtures (RT 10.20-10.32 min) overlapped with the standard 7-HC peak, thereby indicating 7-HC as one of the predominant Phase I metabolites of 7-EC (Fig. 4).

7-HC was metabolized into three polar metabolites, M1 (RT 7.82 min), M2 (RT 8.20 min) and M3 (RT 8.46 min), and two polar metabolites, M1 (RT 6.96 min) and M2 (RT 7.92 min), in rat liver microsomes and liver S9 fractions, respectively (Fig. 5).

The calculated individual organ and total clearance of 7-EC and 7-HC in microsomes and S9 fractions is shown in Tables 2 and 3, and

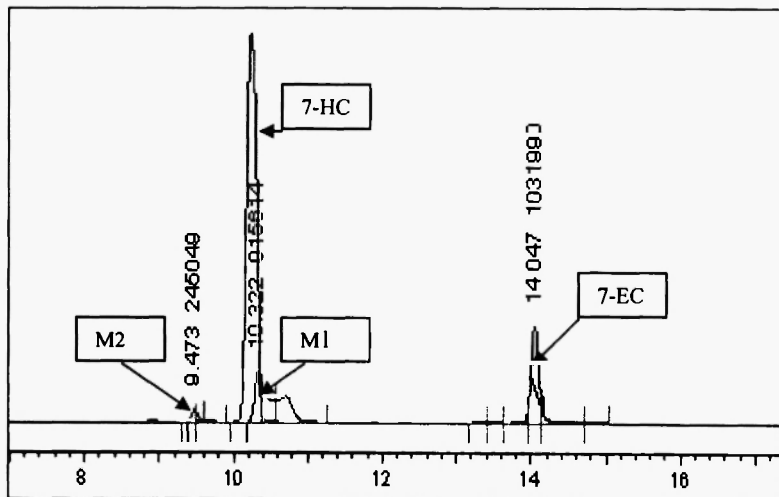


Fig. 4: Representative HPLC chromatogram showing metabolites of 7-ethoxycoumarin (7-EC) formed in rat liver microsomes overlaid with 7-hydroxycoumarin (7-HC) standard. The figure shows formation of two polar metabolites, M1 (retention time [RT] 10.32 min) and M2 (RT 9.47 min) from 7-EC incubation in rat liver microsomes. Overlaying of 7-HC standard indicates 7-HC as one of the predominant metabolite of 7-EC.

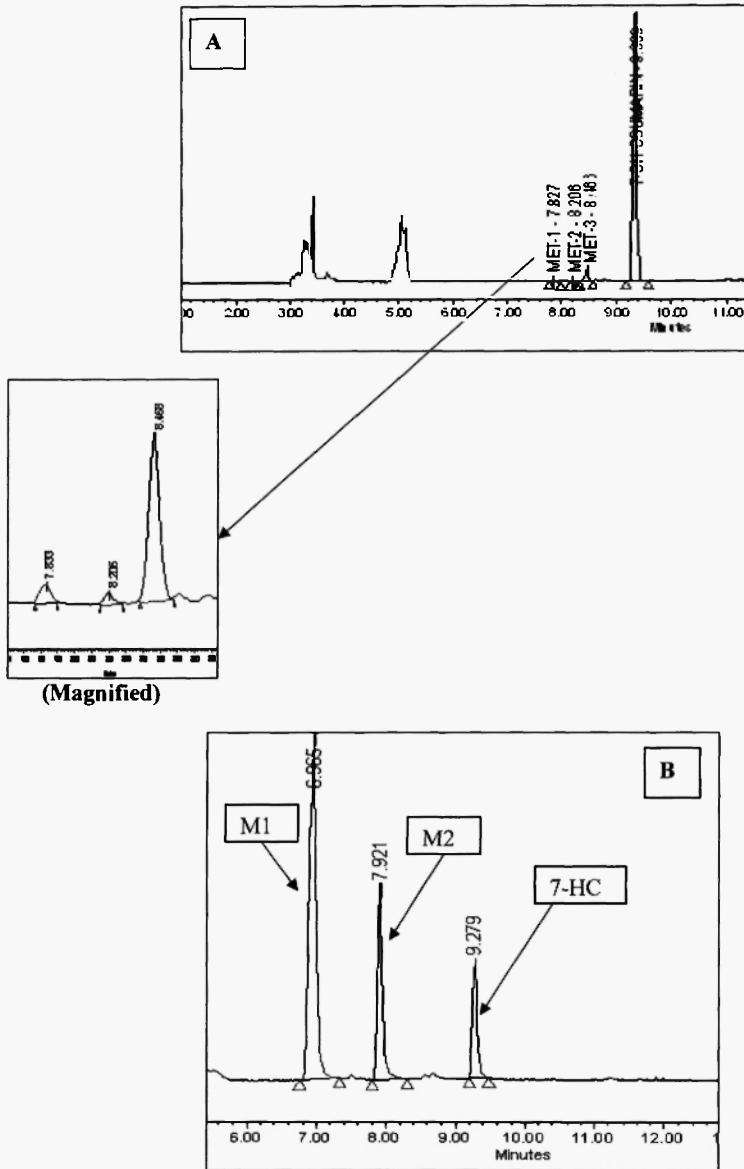


Fig. 5: Representative HPLC chromatogram showing metabolites of 7-hydroxycoumarin (7-HC) formed in rat liver microsomes (A) and S9 fractions (B). The figure shows the formation of three polar metabolites, M1 (retention time [RT] 7.82 min), M2 (RT 8.20 min) and M3 (RT 8.46 min) and two polar metabolites, M1 (RT 6.96 min) and M2 (RT 7.92 min) from 7-HC incubation in rat liver microsomes and S9 fractions.

TABLE 2
In vitro intrinsic clearance estimated for 7-ethoxycoumarin in rat hepatic and extra-hepatic microsomes and S9 fractions

| Organ | Microsomal incubation | | | | S9 fraction incubation | | | | | |
|-----------|----------------------------------|--------------------------------------|---------------------------|----------------------------------|-------------------------|----------------------------------|--------------------------------------|---------------------------|----------------------------------|-------------------------|
| | CL _{int} (μl/min/mg) | CL _{int,org} (μl/min/kg) | Blood flow (ml/min/kg) | CL _{org} (ml/min/kg) | Total CL (ml/min/kg) | CL _{int} (μl/min/mg) | CL _{int,org} (μl/min/kg) | Blood flow (ml/min/kg) | CL _{org} (ml/min/kg) | Total CL (ml/min/kg) |
| Liver | 1.5 | 6986 | 55.2 | 53.3 | | 0.4 | 1680 | 55.2 | 48 | |
| Intestine | 0.1 | 23.2 | 30 | 4.4 | | 0.1 | 23.2 | 30 | 4.4 | |
| Kidneys | 0.2 | 127.4 | 37 | 16 | 78.5 | 0.2 | 158.1 | 37 | 20 | 76.8 |
| Lungs | 0.5 | 182 | 11 | 1.1 | | 0.1 | 24.2 | 11 | 1 | |
| Brain | 0.1 | 58 | 5.2 | 3.7 | | 0.1 | 46.4 | 5.2 | 3.4 | |

Data are presented as mean values ($n = 4$ for each organ).

Blood flow values were obtained from the literature [26,27].

CL_{org} was calculated according to the venous equilibrium model [3].

Total *in vitro* clearance was obtained by adding individual organ clearance values.

CL = clearance; CL_{int} = intrinsic clearance; $CL_{int,org}$ = intrinsic organ clearance; CL_{org} = organ clearance.

TABLE 3
In vitro intrinsic clearance estimated for 7-hydroxycoumarin in rat hepatic and extra-hepatic microsomes and S9 fractions

| Org in | Microsomal incubation | | | | S9 fraction incubation | | | | | |
|-----------|---|---|---|--|--|---|---|--|--|--|
| | CL_{int} ($\mu\text{l}/\text{m in}/\text{mg}$) | $CL_{int,org}$ ($\mu\text{l}/\text{m in}/\text{kg}$) | Bloo f flow ($\text{m l}/\text{m in}/\text{kg}$) | CL_{org} ($\text{m l}/\text{m in}/\text{cg}$) | Total CL ($\text{m l}/\text{m in}/\text{kg}$) | CL_{int} ($\mu\text{l}/\text{m in}/\text{mg}$) | $CL_{int,org}$ ($\mu\text{l}/\text{m in}/\text{kg}$) | Blood flow ($\text{m l}/\text{m in}/\text{kg}$) | CL_{org} ($\text{m l}/\text{m in}/\text{kg}$) | Total CL ($\text{m l}/\text{m in}/\text{kg}$) |
| Liver | 1 | 4123 | 55.2 | 49 | | 3.2 | 14659 | 55.2 | 53.2 | |
| Intestine | 0.1 | 12 | 30 | 1.1 | | 0 | 0.3 | 30 | 0 | |
| Kidneys | 0.2 | 127.4 | 37 | 9.5 | 63.6 | 1.2 | 991 | 37 | 27 | 81.6 |
| Lungs | 0.1 | 36.3 | 1.1 | 1 | | 0 | 6.1 | 1.1 | 0.4 | |
| Brain | 0.2 | 70 | 5.2 | 3 | | 0 | 11 | 5.2 | 1 | |

Data are presented as mean values ($n = 4$ for each organ).
Blood flow values were obtained from the literature [26,27].
 CL_{org} was calculated according to the venous equilibrium model [3].
Total *in vitro* clearance was obtained by adding individual organ clearance values.
 $CL = \text{clearance}$; $CL_{int} = \text{intrinsic clearance}$; $CL_{int,org} = \text{intrinsic organ clearance}$; $CL_{org} = \text{organ clearance}$.

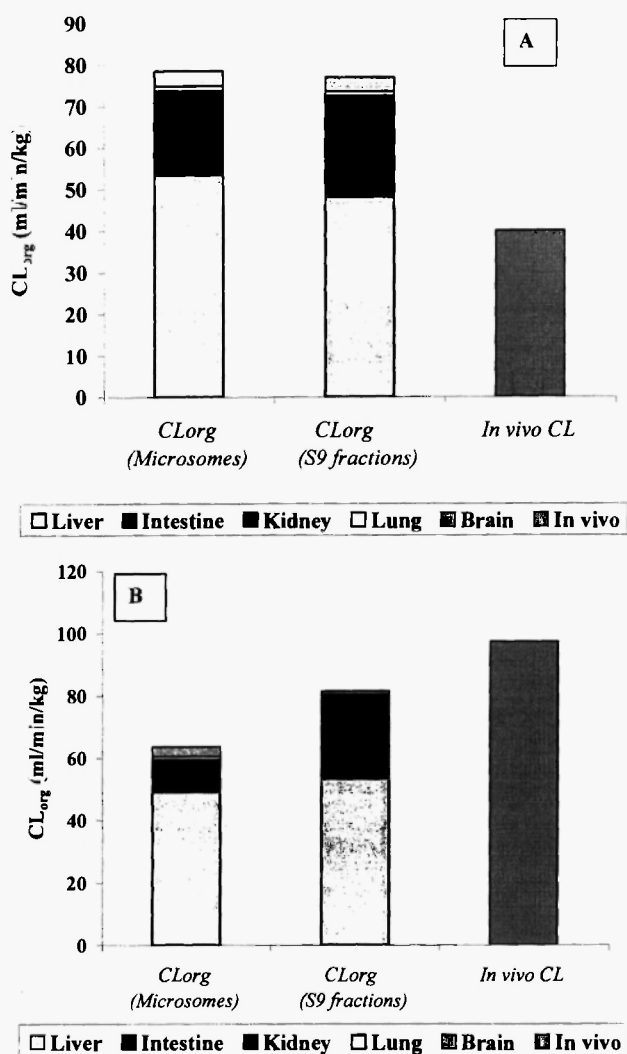


Fig. 6: Total organ clearance of 7-ethoxycoumarin (7-EC) (A) and 7-hydroxycoumarin (7-HC) (B) obtained by scaling of *in vitro* intrinsic clearance in rat hepatic and extra-hepatic microsomes and S9 fractions. Bars showing the mean organ clearance values obtained for 7-EC and 7-HC from incubation studies carried out in duplicate. *In vitro* intrinsic clearance of 7-EC and 7-HC obtained in hepatic and extra-hepatic microsomes and S9 fractions was scaled to organ clearance by using scaling factors and the venous equilibrium model. The total organ clearance (CL_{org}) was determined by adding the individual organ clearance values. The *in vivo* plasma clearance of 7-EC and 7-HC following intravenous administration in rats was obtained from the literature [28,29].

TABLE 4

Comparison of scaled clearance of 7-ethoxycoumarin (7-EC) and 7-hydroxycoumarin (7-HC) to *in vivo* plasma clearance

| Compound | Subcellular fraction | <i>In vitro</i> total CL (ml/min/kg) | <i>In vivo</i> plasma CL* (ml/min/kg) |
|----------|----------------------|---|--|
| 7-EC | Microsomes | 78.5 | 40 |
| | S9 fractions | 76.8 | |
| 7-HC | Microsomes | 63.6 | 97.4 |
| | S9 fractions | 81.6 | |

Total *in vitro* clearance was obtained by adding individual organ clearance values.

* *In vivo* plasma clearance values were obtained from the literature /28,29/.

Figure 6. 7-EC showed a total organ clearance of 78.5 and 76.8 ml/min/kg, and 7-HC showed 63.6 and 81.6 ml/min/kg, by *in vitro* scaling using microsomes and S9 fractions, respectively. Comparison of the *in vitro* total clearance obtained for 7-EC and 7-HC with the corresponding *in vivo* data reported in the literature indicated a slight overprediction for 7-EC and underprediction for 7-HC, as shown in Table 4.

DISCUSSION

In the present study, the drug depletion approach was used to determine the metabolic clearance of two model compounds, 7-EC and 7-HC. These compounds were selected on the basis of their unbound fractions and clearance values in the rat, aiming at a broad range of binding, metabolism and clearance values. Metabolism of xenobiotics is often seen as an exclusive function of the liver, but more recent findings support the notion that the lungs, kidneys and intestine provide a considerable contribution /3/. Therefore, it is important to incorporate not only liver, but also intestine, kidneys, lungs, etc., to predict the overall metabolic clearance. Several *in vitro* models are used to study the metabolism of xenobiotics in hepatic and extra-hepatic organs, each model having its own distinct advantages

and disadvantages. Ideally an *in vitro* model should be simple, applicable in a similar way for each organ, and should also include all metabolic pathways that are defined *in vivo*.

In the present investigation, we used the microsomal and S9 fraction depletion approach, which represents one of the simplest and widely used tools to predict *in vivo* clearance, taking into account that *in vivo* clearance is limited by blood flow and the binding of the substrate to plasma proteins.

Previous studies have reported the investigation of clearance of 7-EC and 7-HC in extra-hepatic tissues using precision-cut slices /3/. In the present study, the hepatic and extra-hepatic clearance of 7-EC and 7-HC was evaluated using subcellular fractions of each tissue. It is known that 7-EC is metabolized to 7-HC by *O*-deethylation, which is catalyzed by CYP1A2 and CYP2E1 enzymes in human liver /31/. Similarly, in rats, CYP2A1 and CYP2A2 are responsible for 7-hydroxylation of 7-EC /32/. The 7-HC formed undergoes Phase II metabolism to form 7-HC-glucuronide and 7-HC-sulfate as the predominant metabolites, along with other previously reported metabolites /33/. Recent work by Ball *et al.* with rat liver slices /18/ indicated that there are several metabolites of 7-EC in addition to 7-HC. Indeed, Jung *et al.* /33/ identified 3-hydroxy-7-ethoxycoumarin as a primary metabolite of 7-EC *in vitro*, and previous work with coumarin in rats showed this closely related chemical to be hydroxylated in several positions, but primarily at position 3 of the lactone ring /34/. Therefore, there are several other metabolites likely to be quantitatively of equal, or more, importance, compared with 7-HC. Thus, UDPGA and PAPS in addition to NADPH were used as co-factors in S9 fraction incubations of 7-EC and 7-HC, since glucuronide and sulfate are predominant metabolites of both drugs in the body along with other reported Phase I metabolites /12,18/.

It was found that the formation rates of 7-HC and other metabolites were greater in hepatic than extra-hepatic microsomes and S9 fractions, which correlates with drug degradation data. The *in vitro* total clearance values obtained for 7-EC were 78.5 and 76.8 ml/min/kg by *in vitro* scaling from microsomes and S9 fractions, respectively. Similarly, for 7-HC, the values were 63.6 and 81.6 ml/min/kg, respectively. For 7-EC, similar *in vitro* clearance values were observed in both microsomes and S9 fractions, which could be due to Phase I metabolism being the primary pathway of metabolism of 7-EC.

However, for 7-HC, S9 fractions showed higher *in vitro* clearance values than microsomes, as it undergoes both Phase I and Phase II metabolism. Therefore, S9 fractions gave a better prediction of *in vivo* clearance.

Previous studies in rat hepatic and extra-hepatic organ tissue slices /3/ have reported the *in vitro* total clearance for 7-HC and 7-EC as 75 and 47 ml/min/kg, respectively, values which are slightly lower and slightly higher than the reported rat *in vivo* plasma clearance values of 97.4 and 40 ml/min/kg, respectively /29,30/. Correlation of our data with these reported values showed similar results; we observed overprediction and underprediction of *in vivo* clearance for 7-EC and 7-HC in both microsomal and S9 fractions. Overprediction may result if enterohepatic circulation occurs *in vivo*. Similarly, underprediction may result if excretion of unchanged drug is a major clearance route in the body. Additional work is required to clarify the cause of these over- and underpredictions. However, the observed clearance was within a 0.5-2 fold range of the *in vivo* values for both 7-EC and 7-HC.

In conclusion, the present study demonstrates the value of an *in vitro* drug depletion assay using S9 and microsomal fractions from hepatic and extra-hepatic tissues for the prediction of *in vivo* clearance. This approach has an obvious advantage when the metabolic fate of the drug under investigation is not known. It also gives important information about the contribution of the various organs towards metabolic clearance. Most importantly, this technique can be applied to human tissues, allowing prediction of metabolic clearance in man in an early phase of drug development.

ACKNOWLEDGEMENTS

The authors D.B. and V.A. are grateful to Piramal Life Sciences Limited for providing all the facilities to carry out this research work.

REFERENCES

1. Yan Z, Caldwell GW. Metabolism profiling and cytochrome P450 inhibition and induction in drug discovery. *Curr Top Med Chem* 2001; 1: 403-425.

2. Nassar A-EF, Kamel AM, Clarimont C. Improving the decision-making process in the structural modification of drug candidates: enhancing metabolic stability. *Drug Discov Today* 2004; 9: 1020-1028.
3. De Graaf IAM, de Kanter R, De Jager MH, et al. Empirical validation of a rat in vitro organ slice model as a tool for in vivo clearance prediction. *Drug Metab Dispos* 2006; 34: 591-599.
4. Griffin SJ, Houston JB. Prediction of in vitro intrinsic clearance from hepatocytes: comparison of suspensions and monolayer cultures. *Drug Metab Dispos* 2005; 33: 115-120.
5. Shimada T, Tsumura F, Yamazaki H. Prediction of human liver microsomal oxidations of 7-ethoxycoumarin and chlorzoxazone with kinetic parameters of recombinant cytochrome P-450 enzymes. *Drug Metab Dispos* 1999; 27: 1274-1280.
6. Skett P, Tyson C, Guillouzo A, Maier P. Report on the international workshop on the use of human in vitro liver preparations to study drug metabolism in drug development. *Biochem Pharmacol* 1995; 50: 280-285.
7. Blaauboer BJ, Boobis AR, Castell JV, et al. The practical applicability of hepatocyte cultures in routine testing: the report and recommendations of ECVAM Workshop 1. *ATLA* 1994; 22: 231-241.
8. Bach PH, Vickers AEM, Fisher R, et al. The use of tissue slices for pharmacotoxicology studies: the report and recommendations of ECVAM Workshop 20. *Altern Lab Anim* 1996; 24: 893-923.
9. Waxman DJ, Lapenson DP, Aoyama T, Gelboin HV, Gonzalez FJ, Korzekwa K. Steroid hormone hydroxylase specificities of eleven cDNA-expressed human cytochrome P450s. *Arch Biochem Biophys* 1991; 290: 160-166.
10. Greenlee WF, Poland A. An improved assay of 7-ethoxycoumarin *O*-deethylase activity: induction of hepatic enzyme activity in C57BL/6J and DBA/2J mice by phenobarbital, 3-methylcholanthrene and 2,3,7,8-tetrachloro-dibenzo-*p*-dioxin. *J Pharmacol Exp Ther* 1978; 205: 596-605.
11. Ryan DE, Levin W. Purification and characterization of hepatic microsomal cytochrome P-450. *Pharmacol Ther* 1990; 45: 153-239.
12. Lake BG. Coumarin metabolism, toxicity and carcinogenicity: relevance for human risk assessment. *Food Chem Toxicol* 1999; 37: 423-453.
13. Boobis AR, Whyte C, Davies SD. Selective induction and inhibition of the components of 7-ethoxycoumarin *O*-deethylase in the rat. *Xenobiotica* 1986; 16: 233-238.
14. Rogiers V, Adriaenssens L, Vandenberghe Y, Gepts E, Callaerts A, Vercruysse A. Critical evaluation of 7-ethoxycoumarin *O*-deethylase activity measurement in intact rat hepatocytes. *Xenobiotica* 1986; 16: 1701-1706.
15. Fry JR, Garle MJ, Lal K. Differentiation of cytochrome P-450 inducers on the basis of 7-alkoxycoumarin *O*-deethylase activities. *Xenobiotica* 1992; 22: 211-215.
16. Bayliss MK, Bell JA, Wilson K, Park GR. 7-Ethoxycoumarin *O*-deethylase kinetics in isolated rat, dog, and human hepatocytes. *Xenobiotica* 1994; 24: 231-241.

17. Worboys PD, Bradbury A, Houston JB. Kinetics of drug metabolism in rat liver slices: rates of oxidation of ethoxycoumarin and tolbutamide, examples of high- and low-clearance compounds. *Drug Metab Dispos* 1995; 23: 393-397.
18. Ball SE, Thiel VE, Tio CO, et al. 7-Ethoxycoumarin metabolism by precision-cut rat hepatic slices. *Drug Metab Dispos* 1996; 24: 383-389.
19. Omura T, Sato R. The carbon monoxide-binding pigment of liver microsomes I. Evidence for its hemoprotein nature. *J Biol Chem* 1964; 239: 2370-2378.
20. Bradford MM. A rapid and sensitive method for the quantitation of microgram quantities of protein utilizing the principle of protein-dye binding. *Anal Biochem* 1976; 72: 248-254.
21. Iyer KR, Sinz MW. Characterization of Phase I and Phase II hepatic drug metabolism activities in a panel of human liver preparations. *Chem Biol Interact* 1999; 118: 151-169.
22. Tassaneeyakul W, Birkett DJ, Veronese ME, et al. Specificity of substrates and inhibitor probes for human cytochromes. *J Pharmacol Exp Ther* 1993; 265: 401-407.
23. Lavhekar SS, Bhopale AK, Lohade AA, Coutinho EC, Iyer KR. Determination of microsomal CYP2A6 activity by high performance liquid chromatography. *Indian J Pharm Sci* 2007; 69: 448-451.
24. Houston JB. Utility of in vitro drug metabolism data in predicting in vivo metabolic clearance. *Biochem Pharmacol* 1994; 47: 1469-1479.
25. De Kanter R, Monshouwer M, Draaisma AL, et al. Prediction of whole-body metabolic clearance of drugs through the combined use of slices from rat liver, lung, kidney, small intestine and colon. *Xenobiotica* 2004; 34: 229-241.
26. Trudeau-Lame ME, Kalgutkar AS, LaFontaine M. Pharmacokinetics and metabolism of the reactive oxygen scavenger α -phenyl-*N*-tert-butyl nitron in the male Sprague-Dawley rat. *Drug Metab Dispos* 2003; 31: 147-152.
27. Davies B, Morris T. Physiological parameters in laboratory animals and humans. *Pharm Res* 1993; 10: 1093-1095.
28. Nakai M, Sasaki M, Okubo S, Yoshioka T, Kunieda T. Intrapulmonary bronchial blood flow of rats as studied by the microsphere method. *Heart Vessels* 1991; 6: 84-89.
29. Carlile DJ, Stevens AJ, Ashforth EI, Waghela D, Houston JB. In vivo clearance of ethoxycoumarin and its prediction from in vitro systems. Use of drug depletion and metabolite formation methods in hepatic microsomes and isolated hepatocytes. *Drug Metab Dispos* 1998; 26: 216-221.
30. Ritschel WA, Johnson RD, Vachharajani NN, Hussain AS. Prediction of the volume of distribution of 7-hydroxycoumarin in man from in vitro and ex vivo data obtained in rat. *Biopharm Drug Dispos* 1992; 13: 389-402.
31. Yamazaki H, Inoue K, Mimura M, Oda Y, Guengerich FP, Shimida T. 7-Ethoxycoumarin *O*-deethylation catalyzed by cytochromes P450 1A2 and 2E1 in human liver microsomes. *Biochem Pharmacol* 1996; 51: 313-319.
32. Honkakoski P, Negishi M. The structure, function, and regulation of cytochrome P450 2A enzymes. *Drug Metab Dispos* 1997; 29: 977-996.

33. Jung B, Graf H, Ullrich V. A new monooxygenase product from 7-ethoxycoumarin and its relation to the *O*-deethylation reaction. *Biol Chem Hoppe-Seyler* 1985; 366: 23-31.
34. Cohen AJ. Critical review of the toxicology of coumarin with special references to interspecies differences in metabolism and hepatotoxic response and their significance to man. *Food Chem Toxicol* 1979; 17: 277-289.